Acta Derm Venereol 2011: 91: 271–278

INVESTIGATIVE REPORT

Role of p38 Mitogen-activated Protein Kinase Isoforms in Murine Skin Inflammation Induced by 12-O-tetradecanoylphorbol 13-acetate

Louise LANGER LILLEHOLT[1], Claus JOHANSEN[1], J. Simon C. ARTHUR[2], Anne FUNDING[1], Bo Martin BIBBY[3], Knud KRAGBALLE[1] and Lars IVERSEN[1]

[1]Department of Dermatology, Aarhus University Hospital, Aarhus, Denmark, [2]MRC Protein Phosphorylation Unit, University of Dundee, Dundee, United Kingdom and [3]Department of Biostatistics, University of Aarhus, Aarhus, Denmark

p38 mitogen-activated protein kinase plays a pivotal role in skin inflammation. The purpose of this study was to investigate the role of the various p38 isoforms. p38β/δ-knockout-C57BL/6 mice were generated, studied in a 12-O-tetradecanoylphorbol 13-acetate (TPA)-induced skin inflammation model and compared with wild-type mice. The inflammatory response was determined by ear thickness, myeloperoxidase activity and histology. mRNA and protein expression of interleukin (IL)-1β and IL-6 was determined by quantitative real-time reverse transcription PCR and enzyme-linked immunoassay. In both groups application of TPA resulted in a significant increase in inflammation, and pretreatment with the p38α/β inhibitor, SB202190 resulted in a significant inhibition. A significantly slower onset but prolonged duration of the response was seen in p38β/δ knockout mice. This was paralleled by a significant, but transient, lower IL-1β and IL-6 protein expression in p38β/δ knockout mice. Although the p38α isoform is important, our data also demonstrate an important role of the p38β and/or δ isoforms in the regulation of TPA-induced skin inflammation. ***Key words: p38 MAPK; knockout mice; inflammation; TPA.***

(Accepted October 18, 2010.)

Acta Derm Venereol 2011; 91: 271–278.

Lars Iversen, Department of Dermatology, Aarhus University Hospital, P. P. Orumsgade 11, DK-8000 Aarhus C, Denmark. E-mail: lars.iversen@ki.au.dk

p38 mitogen-activated protein kinase (p38 MAPK) is a family member of the mitogen-activated protein kinases, which also consists of the extracellular-signal-regulated kinases (ERKs) 1 and 2, ERK5 and Jun N-terminal kinases (JNKs) (1).

p38 is activated by environmental stress, such as hypoxia, oxidative stress, osmotic shock, heat shock, ultraviolet (UV) radiation, and pro-inflammatory cytokines (1, 2). It mediates inflammatory responses through regulation of the gene expression of a number of inflammatory cytokines such as interleukin (IL)-1β, IL-6 and tumour necrosis factor-alpha (TNF-α) (3). This is mediatedthrough different regulatory pathways, including regulation of mRNA stability and translation (4).

Four known isoforms of p38 exist: p38α, p38β, p38δ and p38γ (5). Separate genes encode these isoforms, which share a high degree of homology at the amino-acid level (6–9). *In vitro* studies have shown common substrates, such as activation transcription factor-2 (ATF2) and MAPKAP kinase-2 (MK2) for p38α and p38β (7), whereas p38γ phosphorylates myelin basic protein (MBP) but not ATF2 and MK2, and p38δ phosphorylates MBP and ATF2 but not MK2 (8, 9). Despite a high degree of comparability regarding amino-acid sequence and substrate phosphorylation on serine and/or threonine residues among the various p38 isoforms, they differ in tissue distribution and substrate specificity and each p38 isoform is therefore believed to have a separate and unique function in the cell (6, 8, 9).

p38 activation has been demonstrated in skin inflammation. The p38 as well as the p38α downstream targets, mitogen- and stress-activated protein kinase 1 and 2 (MSK1/2) and MK2 have been found to be activated in lesional psoriatic skin compared with non-lesional psoriatic skin (10–13). p38 activity has also been demonstrated to play a role in contact hypersensitivity (14) and in burn wounds (15). Thus, the p38 signalling pathway exerts both pro- and anti-inflammatory activity.

For instance, we have demonstrated that the p38-activated kinases, MSK1 and 2, are critical in controlling the skin inflammation induced by 12-O-tetradecanoylphorbol 13-acetate (TPA). These findings demonstrate that the p38 signalling pathway plays a dual role in regulating both the magnitude and the duration of an inflammatory response.

Only the p38α, -β and -δ isoforms are expressed in skin (12, 16). In general, p38α and -β are believed to play a role in keratinocytes in response to stress and inflammation, whereas activation of p38δ induces keratinocyte differentiation (17).

Attempts to discriminate the specific role of the various p38 isoforms have been difficult. Most of the available p38 inhibitors block both p38α and p38β, while specific inhibitors of p38γ and δ are not available (18). Furthermore, p38α knockout (KO) mouse are embryonic lethal as a result of placental and vascular defects (19–21). Mice with a cell type-specific p38α KO have

© 2011 The Authors. doi: 10.2340/00015555-1046
Journal Compilation © 2011 Acta Dermato-Venereologica. ISSN 0001-5555

been generated (22), and the role of p38α was studied in different skin inflammation models. An important and cell-type specific role of p38α was demonstrated. The importance of p38α in inflammation has also been demonstrated in a collagen-induced arthritis mouse model using a chemical genetics approach with knock-in mice in which either p38α or p38β was rendered resistant to the effect of specific inhibitors (23).

p38β KO mice have also been generated (24). They were shown to have a normal expression and activation of p38α in response to cellular stress and a normal lipopolysaccharide-induced cytokine production.

Because several studies have demonstrated an important role of p38 in inflammation, a thorough understanding of the role of the various p38 isoforms in the inflammatory response is important. In this study we generated p38β/δ double KO mice and studied TPA-induced skin inflammation in these mice compared with matched controls. Furthermore, we investigated the role of p38 isoforms in the regulation of pro-inflammatory gene expressions at both the transcriptional and translational level.

MATERIALS AND METHODS

Mice

The generation of p38β and p38δ mice has been described previously (24, 25). The double KO of p38β and δ was generated by crossing the two individual single KOs. The mice were viable and fertile and did not exhibit any obvious phenotype when maintained in a pathogen-free environment. Wild-type (WT) C57BL/6 mice and p38β/δ KO mice were received from Taconic Europe (Ry, Denmark). Experiments were conducted in the animal facility of Aarhus University. After shipment, mice were allowed to rest for at least one week before any experiments were conducted. All mice used in this study were 7–9 weeks old. In the ear measurement and myeloperoxidase studies, female mice were used. In the enzyme-linked immunoassay (ELISA), qRT-PCR and histology studies, male mice were used. During the experiments the animals were fed a standard rodent laboratory diet *ad libitum* and had free access to tap water. They were maintained in animal facilities with a temperature of 19–25°C and a 12 h light/dark cycle. While challenging the ears, conducting ear measurements and obtaining punch biopsies the mice were anaesthetized with isoflurane gas, and at the end of the study they were sacrificed by cervical dislocation. All experiments were approved by the Danish Committee for Animal Experiments.

TPA-induced acute skin inflammation

TPA was purchased from Sigma-Aldrich (St Louis, MO, USA) and dissolved in acetone. In a number of experiments p38β/δ KO mice and control C57BL/6 mice were challenged with TPA (0.125 μg/μl) on the ears (2.5 μg/ear). Vehicle studies with acetone alone were also conducted. The p38α/β inhibitor, SB202190, was purchased from Lc Laboratories (Woburn, MA, USA) and dissolved in acetone. Parallel inhibitor experiments with topical application (1 mg/ear) were performed 100 min before TPA challenge. Freshly dissolved solutions of both TPA and SB202190 were made for each experiment. Before challenge (0 h) and at different time points post-challenge (2, 5, 8, 24, 48, 72 h) the ear thickness of the mice was measured using a Mitutyo digimatic indicator.

Myeloperoxidase assays

To determine the degree of neutrophil cell infiltration, myeloperoxidase (MPO) assays were conducted as described previously (26). Four-millimetre punch biopsies were obtained from the ears 8 and 24 h post-challenge and frozen immediately in liquid nitrogen. Then biopsies were placed in 250 μl 0.5% hexadecyltrimethylammonium bromide (HTAB) and homogenized (TissueLyser from Qiagen, Haan, Germany). Homogenates were shaken, incubated at 37°C for 1 h, mixed and centrifuged at 4000 g for 5 min. Twenty μl of the supernatant and 100 μl TMB ONE, Ready-to-use Substrate (Kem-En-Tec Diagnostics A/S, Copenhagen, Denmark) were added to 96-well plates (CM Lab., Vordingborg, Denmark). The plates were incubated at room temperature in the dark while being gently shaken for 10 min. The reaction was then stopped by adding 100 μl 0.2M sulphuric acid (H_2SO_4). Finally, the MPO activity was determined by an ELISA reader (Laboratory Systems iEMS Reader MF, Copenhagen, Denmark) at 450 nm.

A standard curve was constructed with human polymorphonuclear cells obtained from blood of healthy volunteers. Polymorphonuclear cells were prepared using Polymorphprep™ (AXIS-SHIELD PoC AS, Oslo, Norway) according to product instructions.

Isolation of total protein

In a number of experiments the ears were clipped off after sacrificing the mice and immediately placed in liquid nitrogen. The ears were homogenized in 1× cell lysis buffer (20 nM Tris-Base pH 7.5, 150 mM NaCl, 1 mM EDTA, 1 mM EGTA, 1% Triton-X-100, 2.5 mM sodium pyrophosphate, 1 mM β-glycerol phosphate, 1 mM Na_3VO_4, 1 μg ml^{-1} leuleptin and 1 mM phenylmethanesulphonylfluoride (PMSF)) using TissueLyser for 2 × 2 min. After homogenization the samples were left on ice for 10 min before they were sonicated 5 × 10 s. Again the samples were left on ice for 10 min and finally centrifuged at 10,000 g for 10 min at 4°C. The supernatant constitutes the whole-cell protein extract.

Western blotting analysis

Whole-cell protein extracts were prepared from mice ears and equal amounts (as determined in Bradford Protein Assay Protocol) were separated by sodium dodecyl sulphate-polyacrylamide gel electrophoresis (SDS-PAGE) and blotted on to nitrocellulose membranes. Membranes were incubated with either anti-p38α/β MAPK or anti-phospho-p38α/β MAPK (Cell Signalling Technology, Beverly, MA, USA) and detected with horseradish peroxidase (HRP)-conjugated anti-rabbit antibody (DAKO, Glostrup, Denmark) in a standard enhanced chemiluminescence (ECL) reaction (Cell Signalling Technology). A Biotinylated Protein Ladder Molecular Weight Marker (Cell Signalling Technology) was used for estimation of protein size.

Kinase assay

The p38α/β MAPK activity was determined by using a non-radioactive p38 MAP Kinase Assay Kit according to the manufacturer's instructions (Cell Signalling Technology) and as previously described. Briefly, 200 μg of cell lysate was incubated with 20 μl of immobilized phospho-p38α/β MAPK primary antibody overnight at 4°C. The immunocomplexes were isolated and then washed twice with 1 × cell lysis buffer and twice with 1 × kinase buffer (25 mM Tris (pH 7.5), 5 mM β-glycerol phosphate, 2 mM dithiothreitol (DTT), 0.1 mM NA_3VO_4, and 10 mM $MgCl_2$). The pellet was suspended in 1 × kinase buffer supplemented with 200 μM adenosine triphosphate (ATP) and 2 μg of ATF-2 fusion protein and incubated for 30 min at 30°C. The reaction was terminated with 25 μl 3 × SDS Sample buffer and boiled for 5 min. Twenty-five μl of the sample was loaded on SDS-PAGE gel (8–16%).

ELISA

IL-1β and IL-6 expression levels were measured by ELISA using 96-well Maxisorb plates (Invitrogen, Carlsbad, CA, USA) and the DuoSet® ELISA Development System (R&D Systems, Oxon, UK) according to the manufacturer's instructions. Briefly, 100 µl diluted Capture Antibody was added to the wells and incubated overnight at room temperature. The following day the wells were washed before they were blocked for 1 h. The plates were incubated with samples and standards for 2 h at room temperature before they were washed and incubated at room temperature for 2 h with 100 µl diluted Detection Antibody. Finally, 100 µl of streptavidin-HRP were added to the wells. The streptavidin-HRP incubated at room temperature in the dark for 20 min before adding 100 µl of substrate solution (R&D Systems) to the wells. The substrate solution was incubated at room temperature in the dark for 20 min. Finally, the reactions were stopped by adding 50 µl of H_2SO_4 to each well and immediately hereafter the protein expression was determined in doublets by an ELISA reader (Laboratory Systems iEMS Reader MF, Copenhagen, Denmark) at 450 nm.

RNA isolation

To determine mRNA expression, 4 mm punch biopsies were obtained from the mice ears and immediately frozen and stored in liquid nitrogen. Twenty-four hours before RNA extraction samples were submerged in 800 µl RNAlater ICE® (Ambion Inc., Austin, TX, USA) at –80°C for 20 min, and then stored overnight at –20°C. During RNA extraction the biopsies were removed from RNAlater ICE® into fresh tubes and 175 µl SV RNA Lysis Buffer with β-mercaptoethanol was added (SV Total RNA Isolation System, Promega, Madison, WI, USA). The biopsies were then homogenized using TissueLyser. The rest of the RNA extraction procedure, including DNase treatment, was performed according to the manufacturer manual (SV Total RNA Isolation System). The RNA content was determined by spectophotometry (Amersham Pharmacia Biotech, Uppsala, Sweden). Samples were stored at –80°C until quantitative real-time-PCR was performed.

Quantitative real-time reverse transcription PCR

For reverse transcription (RT) Taqman Reverse Transcription Reagents (Applied Biosystems, Foster City, CA, USA) were used including the use of random hexamers as primers. The production of complementary DNA (cDNA) was carried out in a Peltier Thermal Cycler-200 (MJ Research, Inc. Waltham, MA, USA) with three consecutive steps: 10 min incubation (25°C), 30 min reverse transcription (48°C) and 5 min reverse transcriptase inactivation (95°C). The final cDNA was stored at –80°C overnight before real-time PCR was performed.

Primers and probes were obtained from Applied Biosystems. The mRNA expression of IL-1β and IL-6 were determined with Taqman 20X Assays-On-Demand expression assay mix (assay ID: IL-1β: Mm00434228_ml, IL-6: Mm00446190_ml). To normalize the results we used glyceraldehyde 3-phosphate dehydrogenase (GAPDH) (assay ID: Mm99999915_gl) as housekeeping gene. The probes were 6-carboxy-fluorescein-labelled MGP probes.

Each gene was analysed in triplicates and the PCR mastermix used was Taqman 2× Universal PCR Master Mix, No AmpErase from Applied Biosystems. The reactions were carried out in a Rotorgene-3000 real-time PCR machine (Corbett Research, Sydney, Australia) in a volume of 25 µl. The consecutive steps were: 2 min at 50°C, 10 min at 95°C followed by 50 cycles of 15 s at 95°C, and 60 s at 60°C.

Relative gene expression levels were determined using the relative standard curve method (27). Briefly, a standard curve for each gene was made of 5-fold serial dilutions of total RNA from a punch biopsy obtained from the ear of a control mouse known to possess a high RNA content. The curves were then used to calculate the relative amounts of target mRNA in the samples.

Histology

Four-millimetre punch biopsies were obtained from the ears of C57BL/6 control mice before challenge and three times post-challenge (5, 8 and 24 h) and immediately fixed in 4% formaldehyde. Then they were embedded in paraffin and sliced in 4 µm thick sections, mounted onto slides and stained with haematoxylin and eosin in accordance with standard protocols.

Statistical analysis

The ear thickness data were analysed using a linear mixed effects model with treatment, type, time, and the interaction between the three as fixed effects. Mouse and ear (within mouse) were included in the model as random effects. Correlation between measurements on the same ear was taken into account using an unstructured autocorrelation structure.

The MPO, cytokine, and mRNA data were analysed using a linear mixed effects model with type, treatment, and time (and interactions) as fixed effects. Mouse and the interaction between mouse and time were included in the model as random effects. Varying residual variation with treatment groups was taken into consideration in the statistical analysis.

The appropriateness of the models was evaluated by inspecting QQ-plots for the residuals and, in the case of the ear thickness data, by comparing empirical and theoretical autocorrelations. The data were transformed when necessary and results are presented as back-transformed means with 95% confidence intervals.

A significance level of 5% was used and the data were analysed using SAS version 9.2.

RESULTS

TPA-induced p38 activation

In order to demonstrate activation of the p38 signalling pathway, ear biopsies from TPA-treated WT mice were analysed at various time points by phospho-blotting using an antibody recognizing the phosphorylated form of p38. An increase in phosphorylation of p38 was seen at 0.5 h, reaching a maximum 2 h post-challenge and lasting for at least 8 h (Fig. 1a). The increased levels of phosphorylated p38 were paralleled by an increased kinase activity of p38, as measured by ATF2 phosphorylation-induced by immunoprecipitated p38 (Fig. 1b).

Slow onset but prolonged duration of the TPA-induced inflammatory response in p38β/δ knockout mice compared with wild-type mice

The ears of 12 p38β/δ KO mice and 11 WT mice were challenged with 2.5 µg TPA ear^{-1} to induce an inflammatory response. As control, vehicle was applied on the ears of 3 KO mice and 6 WT mice. Thickness of intact ears was measured before challenge (0 h) and 2, 5, 8, 24, 48 and 72 h post-challenge. TPA challenge induced a significant increase in ear thickness in both

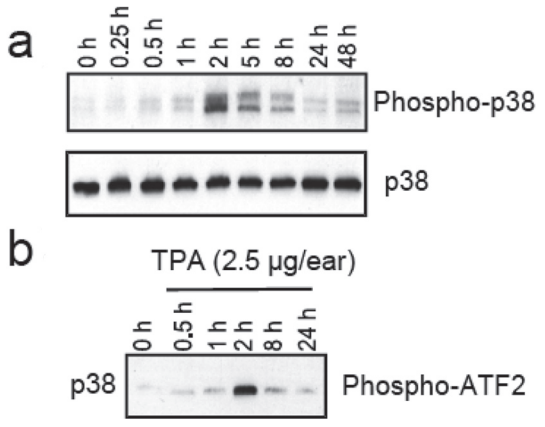

Fig. 1. p38α/β activation in 12-O-tetradecanoylphorbol 13-acetate (TPA)-induced skin inflammation. (a) Whole-cell protein extract was prepared from the mice ears and analysed by Western blotting. Proteins were separated on 8–16% gradient gels and blotted onto a nitrocellulose membrane. After blotting, the membrane was probed with the indicated antibodies. Equal loading was confirmed by incubation with an anti-p38α/β mitogen-activated protein kinase (MAPK) antibody. (b) Whole protein extracts (200 µg of protein) from the mice ears were prepared for immunoprecipitation of p38α/β MAPK. Enzyme activities were determined by an *in vitro* kinase assay, using activation transcription factor-2 (ATF2) as substrate. Kinase reactions were prepared for sodium dodecyl sulphate-polyacrylamide gel electrophoresis (SDS-PAGE), and ATF2 phosphorylation was detected by Western blotting using an anti-phospho-ATF2 antibody. This assay shows the phosphorylation of the phosphorylated p38α/β isoforms. Representative results of (a) three and (b) two separate experiments are shown.

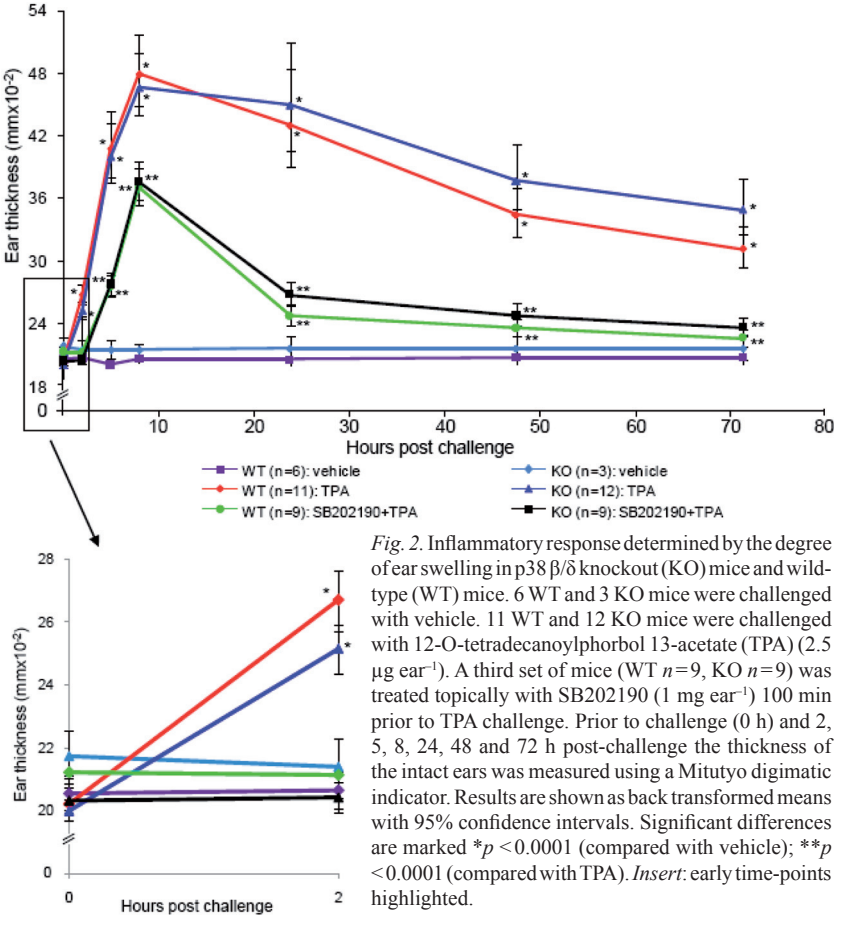

Fig. 2. Inflammatory response determined by the degree of ear swelling in p38 β/δ knockout (KO) mice and wild-type (WT) mice. 6 WT and 3 KO mice were challenged with vehicle. 11 WT and 12 KO mice were challenged with 12-O-tetradecanoylphorbol 13-acetate (TPA) (2.5 µg ear^{-1}). A third set of mice (WT $n=9$, KO $n=9$) was treated topically with SB202190 (1 mg ear^{-1}) 100 min prior to TPA challenge. Prior to challenge (0 h) and 2, 5, 8, 24, 48 and 72 h post-challenge the thickness of the intact ears was measured using a Mitutyo digimatic indicator. Results are shown as back transformed means with 95% confidence intervals. Significant differences are marked *$p<0.0001$ (compared with vehicle); **$p<0.0001$ (compared with TPA). *Insert*: early time-points highlighted.

p38β/δ KO and WT mice compared with vehicle-treated mice ($p<0.0001$ for the interaction between treatment and time). Ear swelling reached a maximum 8 h after TPA challenge in both KO and WT mice (Fig. 2). No significant changes in ear thickness were seen in vehicle-treated mice (Fig. 2). There was no significant difference in ear thickness between KO and WT mice at the beginning of the experiment. A test for no difference between TPA-treated KO and WT mice gave a p-value of 0.005 (2 h: $p=0.01$, 72 h: $p=0.02$, all other time-points had p-values above 0.09). These significant differences demonstrate a slower onset but a prolonged duration of the inflammatory response in KO mice compared with WT mice.

When mice were pretreated with the p38α/β inhibitor, SB202190, a significant inhibition ($p<0.0001$ for the interaction between treatment and time) of the inflammatory response was seen in both WT and KO mice when measured as increase in ear thickness (Fig. 2). Interestingly, a slower onset of the inflammatory response was also seen 2 h after TPA application in SB202190 pretreated KO mice compared with SB202190 pretreated WT mice ($p=0.045$), and a significant increase in ear thickness in SB202190-treated KO mice was seen 24 h after TPA application when compared with WT mice ($p=0.01$). No significant difference was seen after 72 h (Fig. 2).

To assess the degree of neutrophil cell infiltration after TPA-induced inflammation, a myeloperoxidase assay was performed on punch biopsies from mouse ears obtained in a separate set of experiments. There was a significant increase in neutrophil cell infiltration in both p38β/δ KO and WT mice pretreated with vehicle and challenged with TPA compared with mice pretreated with vehicle and challenged with vehicle ($p<0.0001$). This increase was seen both 8 h and 24 h post-challenge (Fig. 3). No significant differences in neutrophil infiltration were seen between p38β/δ KO and WT mice after vehicle pretreatment followed by TPA challenge for 8 and 24 h (8 h: $p=0.702$; 24 h: $p>0.127$) (Fig. 3).

In the myeloperoxidase assay performed on biopsies obtained 8 h post-challenge, pretreatment with SB202190 resulted in a significant inhibition of neutrophil infiltration in both KO and WT mice compared with vehicle plus TPA-treated mice ($p<0.0001$) (Fig. 3a). At 24 h post-challenge there was a significant reduction in neutrophil cell infiltration in WT mice pretreated

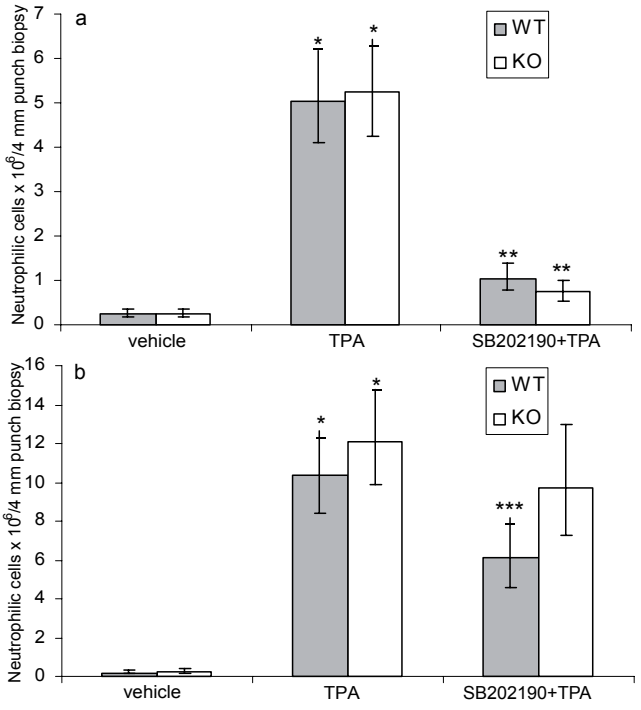

Fig. 3. Measurement of neutrophil cell infiltration in p38 β/δ knockout (KO) mice and wild-type (WT) mice. Three mice in each group were pretreated with vehicle and challenged with vehicle. Ten mice in each group were pretreated with vehicle and challenged with 12-O-tetradecanoylphorbol 13-acetate (TPA). Five mice in each group were pretreated with SB202190 and challenged with TPA. SB202190 was applied topically 100 min prior to TPA challenge. At 8 h (a) and 24 h (b) post-challenge a 4-mm punch biopsy from the ear of each mouse was obtained. Number of neutrophilic cells per 4-mm punch biopsy is shown. Statistical results are shown as back-transformed means with 95% confidence intervals. Significant differences are marked *$p<0.0001$ (compared with vehicle); **$p<0.0001$ (compared with TPA, 8 h); ***$p=0.023$ (compared with TPA, 24 h, WT mice).

with SB202190 before TPA challenge compared with WT mice treated with vehicle before TPA challenge ($p=0.023$) (Fig. 3b). No significant difference was seen between KO mice treated with either vehicle or SB202190 before TPA challenge ($p=0.312$) (Fig. 3b).

When mice were pretreated with SB202190 a higher but statistically insignificant level of neutrophil cell infiltration was seen 24 h after TPA application in p38β/δ KO mice compared with matched WT mice ($p=0.122$) (Fig. 3b).

To visualize the inflammatory response induced by TPA, histological examinations with haematoxylin and eosin staining were conducted. In a separate set of experiments three groups of WT mice were given the following treatments: one group of mice ($n=3$) was pretreated with vehicle 100 min before challenged with vehicle. Another group of mice ($n=6$) was pretreated with vehicle 100 min before challenged with TPA. A third group of mice ($n=6$) was pretreated with SB202190 100 min before challenged with TPA. Four-millimetre punch biopsies were obtained 0, 5, 8 and 24 h post-challenge (Fig. 4). Challenge with TPA resulted in a marked increase in dermal infiltrate and oedema over time (Fig. 4) compared with the ears of mice challenged with vehicle (not shown). Furthermore, the inhibitory effect of SB202190 on the inflammatory response was also confirmed by histological examination (Fig. 4).

TPA-induced IL-1β and IL-6 mRNA expression in p38β/δ knockout mice and wild-type mice

To study the mRNA expression profile of pro-inflammatory cytokines, quantitative real-time RT-PCR was performed on punch biopsies obtained from the ears of the mice.

A significant increase in IL-1β and IL-6 mRNA expression was seen in both KO and WT mice after TPA application ($p<0.0001$ at all time-points compared with vehicle) (Fig. 5a–f). No significant differences were seen in IL-1β and IL-6 mRNA expression between p38β/δ KO mice and WT mice. Pretreatment with SB202190 lead to an inhibition of both IL-1β and IL-6 mRNA expression in both KO and WT mice (Fig. 5a and d). This inhibition was highly significant for both IL-1β and IL-6 mRNA in WT and KO mice after 2 h ($p<0.0001$) whereas the inhibitory effect of SB202190 was less pronounced at the later time-points (Fig. 5b, c, e and f).

TPA-induced IL-1β and IL-6 protein expression in p38β/δ knockout mice compared with wild-type mice

To characterize some of the cytokines involved in the inflammatory response, IL-1β and IL-6 protein expressions were analysed 5, 8 and 24 h post-challenge.

The induction of IL-1β was significant 5, 8 and 24 h after TPA challenge in both KO and WT mice compared with the vehicle challenged mice ($p<0.0001$ at all time-

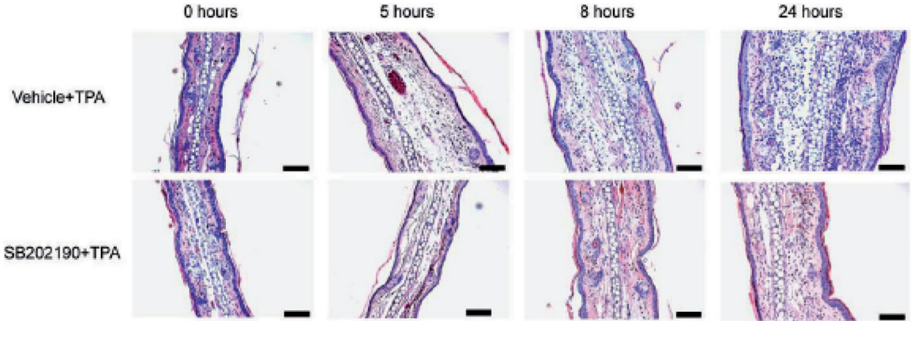

Fig. 4. Histological sections obtained from wild-type (WT) mice showing the effects of 12-O-tetradecanoylphorbol 13-acetate (TPA) challenge with and without pretreatment with SB202190. Haematoxylin and eosin (H&E) stained histological sections of WT mice ears pretreated with vehicle prior to TPA challenge (*upper panel*, bar=100 μm) and WT mice ears pretreated with SB202190 prior to TPA challenge (*lower panel*, bar=100 μm). Different time points are shown: 0 h (prior to challenge) and 5, 8 and 24 h post-challenge. Representative transversal sections of mice ears are shown. $n=3$ for each treatment group.

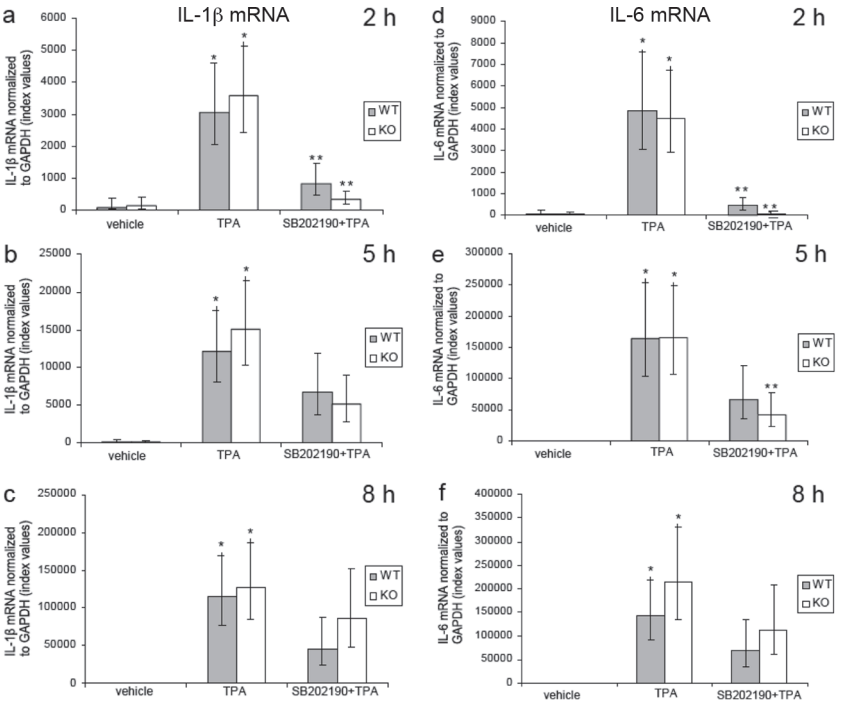

Fig. 5. 12-O-tetradecanoylphorbol 13-acetate (TPA)-induced IL-1β and IL-6 mRNA expression in p38β/δ knockout (KO) mice compared with wild-type (WT) mice. In two separate experiments 4-mm punch biopsies were obtained 2, 5 and 8 h post-challenge and interleukin (IL)-1β and IL-6 mRNA expressions were analysed by quantitative real-time reverse transcription polymerase chain reaction (real-time RT-PCR) and normalized to glyceraldehyde-3-phosphate dehydrogenase (GAPDH). In the first experiment two biopsies was obtained 2 h post-challenge from the left ear and another two biopsies was taken 5 h post-challenge from the right ear. In the second experiment only two biopsies 8 h post-challenge was obtained from each mouse. In each experiment the KO mice and WT mice were divided into the following groups: 3 mice received pretreatment with vehicle prior to challenge with vehicle. 10 mice received pretreatment with vehicle prior to challenge with TPA. Five mice received pretreatment with SB202190 prior to challenge with TPA. In all experiments pretreatment was applied topically 100 min prior to challenge. The graphs show indexed values of mRNA expression compared with vehicle-pretreated and vehicle-challenged WT mice. (a) IL-1β, 2 h (b) IL-1β, 5 h (c) IL-1β, 8 h (d) IL-6, 2 h (e) IL-6, 5 h (f) IL-6, 8 h. Results are shown as back-transformed means with 95% confidence intervals. Significant differences are marked *$p<0.0001$ (compared with vehicle); **$p<0.0001$ (compared with TPA). Note that the y-axes have different scales in each sub-figure.

points). The IL-1β protein expression was maximal 8 h post-challenge (Fig. 6a–c). When SB202190 pretreatment was applied, a significant ($p<0.0036$ in all cases) reduction in IL-1β protein expression was seen in both mouse groups 5, 8, and 24 h post-challenge. Interestingly a statistically significant lower IL-1β expression was seen in p38β/δ KO mice compared with WT mice 8 h after TPA challenge ($p=0.0003$). Twenty-four hours after TPA challenge no statistically significant difference was seen in IL-1β expression between WT mice and p38β/δ KO mice (Fig. 6a–c).

Induction of IL-6 was similar to IL-1β induction. TPA-challenge resulted in a significant increase in IL-6 protein expression 5, 8 and 24 h post-challenge in both p38β/δ KO and WT mice ($p<0.0001$ in all cases compared with vehicle). The maximal expression was 8 h post-challenge (Fig. 6d–f). When SB202190 pretreatment was applied a significant inhibition of IL-6 protein expression occurred

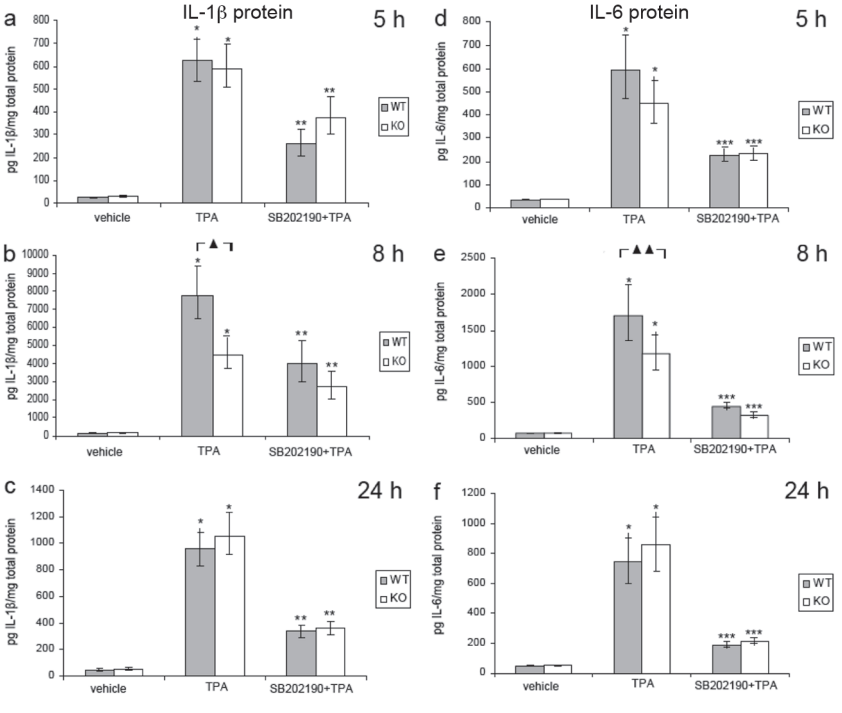

Fig. 6. 12-O-tetradecanoylphorbol 13-acetate (TPA)-induced IL-1β and IL-6 protein expression in p38β/δ knockout (KO) mice and wild-type (WT) mice. In three separate experiments mouse ears were collected 5, 8 and 24 h post-challenge immediately after the mouse was sacrificed and IL-1β and IL-6 protein expression was determined by enzyme-linked immunoassay (ELISA). In each experiment the KO mice and WT mice were divided into the following groups: 3 mice received pretreatment with vehicle prior to challenge with vehicle. Ten mice received pretreatment with vehicle prior to challenge with TPA. Five mice received pretreatment with SB202190 prior to challenge with TPA. In all experiments pretreatment was applied topically 100 min prior to challenge. (a) IL-1β, 5 h (b) IL-1β, 8 h (c) IL-1β, 24 h (d) IL-6, 5 h (e) IL-6, 8 h (f) IL-6, 24 h. Results are shown as back-transformed means with 95% confidence intervals. Significant differences are marked *$p<0.0001$ (compared with vehicle); **$p<0.0036$ (compared with TPA); ***$p<0.0001$ (compared with TPA); ▲$p=0.0003$; ▲▲$p=0.022$. Note that the y-axes have different scales in each sub-figure.

in both mouse groups ($p < 0.0001$). As seen with IL-1β, a significantly higher expression level of IL-6 protein was seen in WT mice compared with KO mice 8 h after challenge with TPA ($p = 0.022$).

DISCUSSION

While p38β KO and p38δ KO mice have been described previously (24, 25), p38β/δ double KO mice were generated for the first time in this study. p38β/δ KO mice were viable and fertile and they developed normally.

p38β has been shown to play a role in keratinocytes in response to stress and inflammation, whereas p38δ may play a role in keratinocyte differentiation (17) and p38δ has also been shown to be essential for skin tumour development in mice (28).

Several mouse models have been established to study skin inflammation (29) including various delayed allergy reactions and different non-allergic toxic skin inflammatory models. In this study the role of the various p38 isoforms were studied in a non-allergic TPA-induced skin inflammation model using both p38β/δ KO mice and WT control mice.

TPA application resulted in a significant increase in ear thickness and neutrophil cell infiltration in both WT and KO mice and pretreatment with the p38α/β inhibitor, SB202190, before TPA application resulted in a significant inhibition of the inflammatory response in both mouse groups. However, a significant slower onset but prolonged duration of the TPA-induced inflammatory response was seen in p38β/δ KO mice compared with WT mice, and this was paralleled by a significant lower IL-1β and IL-6 protein expression in p38β/δ KO mice compared with WT mice 8 h after TPA application, whereas no differences were seen at 24 h. The reason why the IL-1β and IL-6 protein expression was significantly reduced in the KO mice at 8 h, but only insignificantly reduced at 5 h, is probably due to the fact, that the protein expression at 8 h were substantially higher, which makes the difference easier to detect.

Normal epidermal keratinocytes express p38α, p38β and p38δ (12, 16). p38γ has not been detected in keratinocytes or inflammatory cell lineages (6, 12, 16) and is unlikely to play a role in skin inflammation although p38γ expression has been demonstrated in human fibroblasts (30). p38α is therefore the dominating p38 isoform in the epidermis of p38β/δ KO mice and when the p38α/β inhibitor, SB202190, was applied to the skin of p38 β/δ KO mice before TPA challenge, p38γ was the only active p38 isoform present. The maximal inflammatory response obtained 8 h after TPA application was similar in p38β/δ KO mice and WT mice. Furthermore, the inhibition of the inflammatory response after pretreatment with SB202190 was similar in the two groups. This allows us to conclude that the p38α is the most important p38 isoform in skin inflammation which is also in accordance with previous reports (22). Homozygous p38α KO mice are not viable (20), whereas homozygous p38β KO mice were viable and p38β KO mice were shown to have a normal activation of p38 in response to cellular stress and a normal lipopolysaccharide-induced cytokine production (24). In contrast, homozygous p38α KO embryonic stem cells showed no IL-6 production in response to IL-1 stimulation (20), supporting a dominating role of the p38α isoform in an inflammatory response. Using a contact hypersensitivity model, heterozygous p38α KO mice were also shown to have reduced 1-fluoro-2,4-dinitrobenzene (DNFB)-induced ear swelling and infiltration of cells compared with WT mice (14).

The dominating role of p38α in eliciting inflammatory responses is not limited to the skin. A dominating role of p38α in collagen-induced arthritis in mice has also been demonstrated (23). These results are consistent with our findings and indicate a key role of p38α in inflammatory responses in general. Our data also demonstrate a minor role of p38β and/or δ in the TPA-induced inflammatory response. A significant slower onset, but prolonged duration, of the TPA-induced inflammatory response was seen in p38β/δ KO mice compared with WT mice, and this difference between KO and WT mice was maintained when both p38α and β were inhibited by SB202190, suggesting a role of p38δ in this response, although our results cannot exclude that the observed changes seen in the KO mice is the net result of opposite responses of p38 β and δ. Opposite regulatory effects of p38 isoforms have been demonstrated previously (31). However, it is also possible, that application of SB202190 did not result in complete inhibition of p38α and β, and therefore, a role of p38β cannot be excluded. Schindler et al. (28) have shown previously that loss of p38δ prevented TPA-induced epidermal hyperproliferation and lead to reduced ERK and AP-1 activation supporting a role of this p38 isoform in TPA-induced inflammatory responses. Although a definite conclusion cannot be drawn based on the data presented here, our observation indicates a dual activity of p38β and/or δ in the inflammatory response. In the initial phase of an inflammatory response p38β and/or δ seem to exert pro-inflammatory activity, whereas a role in terminating the inflammatory response may be dominating in the later stages. Interestingly, a dual activity in an inflammatory response has previously been demonstrated for p38α (22) as well as for the p38α downstream kinase MSK1 and 2 (32). The slower onset of the inflammatory response seen in p38 β/δ KO mice can in part be explained by the decreased IL-1β protein expression seen after 8 h. Because no differences between p38β/δ KO and WT mice were seen in IL-1β mRNA expression at any timepoints, our data indicate a role of p38β and/or δ in the post-transcriptional regulation of IL-1β expression.

Our results, together with previously published data demonstrating a dual activity of the p38 isoforms, illustrate the need for a deeper understanding of the

signalling pathways that control the expression of pro-inflammatory cytokines and how they are integrated in the inflammatory process in order to point out which kinases are likely to be the best therapeutic targets.

It is indisputable that the p38 signalling pathway plays an important role in eliciting inflammatory responses, but kinases downstream of p38 may turn out to be better drug targets. It is important to consider these questions when planning future strategies for pharmacological inhibition of the p38 signalling pathway.

REFERENCES

1. Ashwell JD. The many paths to p38 mitogen-activated protein kinase activation in the immune system. Nat Rev Immunol 2006; 6: 532–540.
2. Roux PP, Blenis J. ERK and p38 MAPK-activated protein kinases: a family of protein kinases with diverse biological functions. Microbiol Mol Biol Rev 2004; 68: 320–344.
3. Ono K, Han J. The p38 signal transduction pathway: activation and function. Cell Signal 2000; 12: 1–13.
4. Zarubin T, Han J. Activation and signaling of the p38 MAP kinase pathway. Cell Res 2005; 15: 11–18.
5. Kyriakis JM, Avruch J. Mammalian mitogen-activated protein kinase signal transduction pathways activated by stress and inflammation. Physiol Rev 2001; 81: 807–869.
6. Hale KK, Trollinger D, Rihanek M, Manthey CL. Differential expression and activation of p38 mitogen-activated protein kinase alpha, beta, gamma, and delta in inflammatory cell lineages. J Immunol 1999; 162: 4246–4252.
7. Jiang Y, Chen C, Li Z, Guo W, Gegner JA, Lin S, et al. Characterization of the structure and function of a new mitogen-activated protein kinase (p38beta). J Biol Chem 1996; 271: 17920–17926.
8. Kumar S, McDonnell PC, Gum RJ, Hand AT, Lee JC, Young PR. Novel homologues of CSBP/p38 MAP kinase: activation, substrate specificity and sensitivity to inhibition by pyridinyl imidazoles. Biochem Biophys Res Commun 1997; 235: 533–538.
9. Li Z, Jiang Y, Ulevitch RJ, Han J. The primary structure of p38 gamma: a new member of p38 group of MAP kinases. Biochem Biophys Res Commun 1996; 228: 334–340.
10. Funding AT, Johansen C, Kragballe K, Otkjaer K, Jensen UB, Madsen MW, et al. Mitogen- and stress-activated protein kinase 1 is activated in lesional psoriatic epidermis and regulates the expression of pro-inflammatory cytokines. J Invest Dermatol 2006; 126: 1784–1791.
11. Funding AT, Johansen C, Gaestel M, Bibby BM, Lilleholt LL, Kragballe K, et al. Reduced oxazolone-induced skin inflammation in MAPKAP kinase 2 knockout mice. J Invest Dermatol 2009; 129: 891–898.
12. Johansen C, Kragballe K, Westergaard M, Henningsen J, Kristiansen K, Iversen L. The mitogen-activated protein kinases p38 and ERK1/2 are increased in lesional psoriatic skin. Br J Dermatol 2005; 152: 37–42.
13. Johansen C, Funding AT, Otkjaer K, Kragballe K, Jensen UB, Madsen M, et al. Protein expression of TNF-alpha in psoriatic skin is regulated at a posttranscriptional level by MAPK-activated protein kinase 2. J Immunol 2006; 176: 1431–1438.
14. Takanami-Ohnishi Y, Amano S, Kimura S, Asada S, Utani A, Maruyama M, et al. Essential role of p38 mitogen-activated protein kinase in contact hypersensitivity. J Biol Chem 2002; 277: 37896–37903.
15. Ipaktchi K, Mattar A, Niederbichler AD, Hoesel LM, Hemmila MR, Su GL, et al. Topical p38MAPK inhibition reduces dermal inflammation and epithelial apoptosis in burn wounds. Shock 2006; 26: 201–209.
16. Dashti SR, Efimova T, Eckert RL. MEK7-dependent activation of p38 MAP kinase in keratinocytes. J Biol Chem 2001; 276: 8059–8063.
17. Eckert RL, Efimova T, Balasubramanian S, Crish JF, Bone F, Dashti S. p38 Mitogen-activated protein kinases on the body surface – a function for p38 delta. J Invest Dermatol 2003; 120: 823–828.
18. Karaman MW, Herrgard S, Treiber DK, Gallant P, Atteridge CE, Campbell BT, et al. A quantitative analysis of kinase inhibitor selectivity. Nat Biotechnol 2008; 26: 127–132.
19. Adams RH, Porras A, Alonso G, Jones M, Vintersten K, Panelli S, et al. Essential role of p38alpha MAP kinase in placental but not embryonic cardiovascular development. Mol Cell 2000; 6: 109–116.
20. Allen M, Svensson L, Roach M, Hambor J, McNeish J, Gabel CA. Deficiency of the stress kinase p38alpha results in embryonic lethality: characterization of the kinase dependence of stress responses of enzyme-deficient embryonic stem cells. J Exp Med 2000; 191: 859–870.
21. Mudgett JS, Ding J, Guh-Siesel L, Chartrain NA, Yang L, Gopal S, et al. Essential role for p38alpha mitogen-activated protein kinase in placental angiogenesis. Proc Natl Acad Sci USA 2000; 97: 10454–10459.
22. Kim C, Sano Y, Todorova K, Carlson BA, Arpa L, Celada A, et al. The kinase p38 alpha serves cell type-specific inflammatory functions in skin injury and coordinates pro- and anti-inflammatory gene expression. Nat Immunol 2008; 9: 1019–1027.
23. O'Keefe SJ, Mudgett JS, Cupo S, Parsons JN, Chartrain NA, Fitzgerald C, et al. Chemical genetics define the roles of p38alpha and p38beta in acute and chronic inflammation. J Biol Chem 2007; 282: 34663–34671.
24. Beardmore VA, Hinton HJ, Eftychi C, Apostolaki M, Armaka M, Darragh J, et al. Generation and characterization of p38beta (MAPK11) gene-targeted mice. Mol Cell Biol 2005; 25: 10454–10464.
25. Sabio G, Arthur JS, Kuma Y, Peggie M, Carr J, Murray-Tait V, et al. p38gamma regulates the localisation of SAP97 in the cytoskeleton by modulating its interaction with GKAP. EMBO J 2005; 24: 1134–1145.
26. Bradley PP, Priebat DA, Christensen RD, Rothstein G. Measurement of cutaneous inflammation: estimation of neutrophil content with an enzyme marker. J Invest Dermatol 1982; 78: 206–209.
27. Otkjaer K, Kragballe K, Funding AT, Clausen JT, Noerby PL, Steiniche T, et al. The dynamics of gene expression of interleukin-19 and interleukin-20 and their receptors in psoriasis. Br J Dermatol 2005; 153: 911–918.
28. Schindler EM, Hindes A, Gribben EL, Burns CJ, Yin Y, Lin MH, et al. p38delta mitogen-activated protein kinase is essential for skin tumor development in mice. Cancer Res 2009; 69: 4648–4655.
29. Gudjonsson JE, Johnston A, Dyson M, Valdimarsson H, Elder JT. Mouse models of psoriasis. J Invest Dermatol 2007; 127: 1292–1308.
30. Kwong J, Hong L, Liao R, Deng Q, Han J, Sun P. p38alpha and p38gamma mediate oncogenic ras-induced senescence through differential mechanisms. J Biol Chem 2009; 284: 11237–11246.
31. Askari N, Diskin R, Avitzour M, Capone R, Livnah O, Engelberg D. Hyperactive variants of p38alpha induce, whereas hyperactive variants of p38gamma suppress, activating protein 1-mediated transcription. J Biol Chem 2007; 282: 91–99.
32. Ananieva O, Darragh J, Johansen C, Carr JM, McIlrath J, Park JM, et al. The kinases MSK1 and MSK2 act as negative regulators of Toll-like receptor signaling. Nat Immunol 2008; 9: 1028–1036.